
MHD Micropolar Fluid Flow Over a Permeable Stretching Sheet in the presence of Variable Viscosity and Thermal Conductivity with Soret and Dufour Effects.

E. O. Fatunmbi^{1*} and O. J. Fenuga²

^{1*} Department of Mathematics and Statistics, Federal Polytechnic, Ilaro, Nigeria.

² Department of Mathematics, University of Lagos, Nigeria

*Corresponding author: olusojiephesus@yahoo.com

Article Info

Received: 13 November 2017 Revised: 13 December 2017

Accepted: 27 December 2017 Available online: 31 January 2018

Abstract

This study investigated the heat and mass transfer behaviour of thermally radiating and chemically reacting MHD Micropolar fluid over a permeable stretching sheet in a Darcy-Forchheimer porous medium under the influence of temperature dependent viscosity and thermal conductivity. The effects of Soret and Dufour in the presence of non-uniform heat source/sink are also examined. The coupled nonlinear partial differential equations governing the fluid flow are transformed into coupled nonlinear ordinary differential equations by applying Lie-group scaling transformations. The resulting coupled nonlinear ODEs are solved by means of Weighted residuals method (WRM) and the obtained solution compared with shooting technique alongside fourth order Runge-Kutta method. The influences of the emerging flow parameters on the dimensionless velocity, microrotation, temperature and species concentration profiles are graphically presented while the effects of some selected flow parameters on the skin friction coefficient, wall couple stress, heat and mass transfer rates are tabulated.

Keywords: Dufour effect; Lie-group scaling; Micropolar fluid; Soret effect; Weighted residuals method.

MSC2010: 76S05, 76W05

1 Introduction

In the recent times, the study of non-Newtonian fluids has gain considerable attention from engineers and researchers owing to the increasing significance and practical relevance of these fluids in many industrial processes. A nonlinear relationship between the shear stress and the shear rate describe the flow dynamics of non-Newtonian fluids, these fluids offer great applications in the engineering and manufacturing processes, such as in polymer engineering, petroleum drilling, food processing manufacturing and many others. Complex rheological behaviour that fluids exhibit at micro and nano scales cannot be adequately captured by the classical continuum theories, at such, various microcontinuum theories have been formulated such as simple microfluids, simple deformable directed fluids, polar fluids, anisotropic fluids and micropolar fluids.

Prominent among the non-Newtonian fluids models is the micropolar fluids theory introduced by Eringen [1] and extended to thermo-micropolar fluids also by Eringen [2]. These are fluids with microstructures. The concept of micropolar fluid deals with a class of fluids that exhibit certain microscopic effect arising from the local structure and micromotion of the fluid element. Such fluids are of a complex nature and individual fluid particles may be of different shapes and may shrink and/or expand, occasionally changing shapes and rotating independently of the rotational movement of the fluid Lukaszewicz [3]. Physically, micropolar fluids may represent fluids consisting of rigid, randomly oriented (or spherical) particles suspended in a viscous medium, where particles deformation is ignored, they belong to the group of fluids with non-symmetric stress tensor that are called polar fluids which constitute a substantial generalization of the Navier-Stokes model. These fluids offer a mathematical model for investigating the flow of complex and complicated fluids such as suspension solution, animal blood, liquid crystals, polymeric fluids and clouds with dust (Ahmadi, [4]; Hayat *et al.*, [5]).

The boundary layer flow of such fluids were first studied by Peddieson and McNitt [6], thereafter, several authors have investigated these fluids on different geometries and conditions. The boundary layer flow past stretching sheet is found applicable in engineering processes such as extrusion of plastic sheet, glass blowing, textile and paper production. The pioneering work on linearly stretching sheet was carried out by Crane [7] who gave the a similarity solution in closed analytical form for the steady two-dimensional problem. Gupta & Gupta [8] extended the work of Crane to include heat and mass transfer on stretching sheet with suction or blowing. Eldabe *et al.*, [9] studied MHD flow of a micropolar fluid past a stretching sheet with heat transfer. Elbashbeshy and Bazid [10] examined heat transfer over a stretching sheet embedded in a porous medium.

The boundary layer flow and heat transfer of an electrically conducting fluid over stretching surfaces is of practical applications in manufacturing and engineering operations such as hot rolling, wire drawing, the extrusion of polymer sheet from a die and the cooling of metallic sheets. In such processes, the properties of the end products depend to some extent on the kinematics of stretching and the simultaneous rate of heating and cooling during the fabrication processes. Hence, the rate of cooling can be controlled by the use of electrically conducting fluid and the application of magnetic field. To this end, Kumar [11] numerically studied the problem of heat and mass transfer in a hydromagnetic flow of a micropolar fluid past a stretching sheet using the Finite element technique. The author reported that the fluid velocity increased with a rise in the material parameter while the opposite was the case with increase in the magnetic field parameter. Similarly, microrotation, concentration and temperature were increasing functions of magnetic field parameter.

The influence of thermo-diffusion (Soret) and diffusion-thermo (Dufour) on fluids which have higher temperature and concentration gradients cannot be ignored, because when heat and mass transfer occur simultaneously in a moving fluid the relations between the fluxes and the driving potentials are of intricate nature. Observation has shown that energy flux can be produced not only by temperature gradient but also by concentration gradient, such effect is termed as diffusion-thermo/Dufour effect. In like manner, mass flux caused by temperature gradient is termed as thermo-diffusion/Soret effect. These terms have been mostly neglected by researchers on the basis that they have less magnitude than the effects described by Fourier and Ficks laws. The applications of these effects are found useful in the study of hydrology, petrology and geosciences. In consequence, Hayat *et al.*, [12] investigated the influence of Soret and Dufour on stagnation point flow of a micropolar fluid toward a linear stretching horizontal surface. The governing partial differential equations of the fluid flow were transformed into ordinary differential equations by similarity transformations and then solved by the Homotopy Analysis Method (HAM). The effects of Prandtl number, material parameter, Dufour number and Soret parameters on the velocity, temperature and concentration distribution were found to be significant on the model. Similarly, Reddy and Chamkha [13] reported Soret and Dufour effects on MHD heat and mass transfer flow of a micropolar fluid, Srinivasacharya *et al.*, [14] studied

Soret and Dufour effects on MHD free convection in a micropolar fluid, Srinivasacharya and RamReddy [15] investigated Soret and Dufour effects on mixed convection in a non-Darcy porous medium saturated with micropolar fluids. Mishra *et al.*, [16] investigated chemical reaction and Soret effects on hydromagnetic micropolar fluid along a stretching sheet. Similarity transformation technique was used to transform the governing PDEs into ODEs while Runge-Kutta integration scheme alongside shooting method was used to solve the nonlinear ODEs.

Flow and heat transfer in Porous media with heat sources are widely applicable in high temperature heat exchangers, cooling of underground electric cables, recovery of petroleum resources, geothermal energy extractions etc. To this end, Mohammed and Abo-Dahab [17] investigated heat and mass transfer in MHD micropolar flow over a vertical moving porous plate in a porous medium with heat generation using perturbation technique. The authors reported that the translational velocity across the boundary layer and the magnitude of microrotation at the wall are decreased with an increase in the values of magnetic, Schmidt and Prandtl parameters while the trend was reversed with an increase in the values of radiation, thermal Grashof and solutal Grashof parameters. Other researchers who have studied boundary layer flow in porous media with heat sources include Olajuwon *et al.*, [18]; Jat *et al.*, [19] and Pal and Chatterjee, [20]. Many of the engineering and manufacturing operations occur at high temperature, thus, the effect of thermal radiation on magnetohydrodynamic flow, heat and mass transfer becomes very important for the design of pertinent equipment such as the design of fins, steel rolling, nuclear power plants, electric power generation and solar power technology. Due to this many researchers have reported the influence of thermal radiation on fluid flow (Ibrahim, [21]; Hamad *et al.* [22]; Mukhopadhyay, [23]).

Fluid flows involving chemical reaction have important applications in many engineering processes such as drying evaporation at the surface of a water body, food processing, smog formation, groves of fruit trees and crop damage due to freezing. Chemical reaction can be of two types: homogeneous reaction which is analogous to internal source of heat generation, it occurs uniformly throughout a given phase. On the other hand heterogeneous reaction occurs in a restricted region or within the boundary of a phase, thus it can be considered as a boundary condition such as the constant heat flux in heat transfer. In most situations of practical chemical reactions, the rate of reaction depends on the concentration of the species itself, a first order reaction occurs if the rate of the reaction is directly proportional to the concentration. Such study has attracted researchers such as (Ibrahim, [21]; Kandasamy *et al.*, [24]).

Many researchers assumed constant fluid properties, however, physical properties of fluid may change largely with temperature. The increase in temperature enhances the transport phenomena by decreasing the viscosity across the momentum boundary layer such that the rate of heat transfer at wall is affected, similarly, a decrease in fluid viscosity can make the fluid velocity decrease appreciably with an increase in transverse distance from a stretching plate. Hence, to predict the flow behaviour accurately, it is important to consider the variation of viscosity and thermal conductivity. Pal and Mondal [25] reported the effects of temperature-dependent viscosity and variable thermal conductivity on Newtonian fluid. The effects of radiation and variable fluid viscosity on stagnation point flow past a porous stretching sheet was examined by Mukhopadhyay [23].

The aim of this study is to investigate MHD heat and mass transfer in a thermally radiating and chemically reacting micropolar fluid over a vertical permeable stretching sheet in a Darcy-Forchheimer porous medium with non-uniform heat source/sink, with Soret and Dufour effects under the influence of variable viscosity and thermal conductivity. Instead of using similarity transformations directly from the literature, similarity variables were developed using the Lie group scaling analysis. The similarity variables developed were applied to transform the governing PDEs to ODEs and the resulting nonlinear equations were solved by a semi-analytic method known as Weighted residuals method (WRM).

2 Mathematical formulation of the problem

Consider steady two-dimensional, viscous, incompressible, electrically conducting, thermally radiating and chemically reactive micropolar fluid past a vertical permeable stretching plate embedded in a fluid saturated Darcy-Forchheimer porous medium. A uniform magnetic field of strength B_0 is imposed normal to the flow direction in which (\bar{y}, \bar{z}) depicts the transverse and vertical coordinates with corresponding velocity components (\bar{v}, \bar{w}) as depicted in Fig.1 The induced magnetic field due to the motion of the electrically conducting fluid is negligible. Also, it is assumed that the external electric field is zero and the field due to polarization of charges is negligible. The magnetic Reynolds number is assumed to be small such that the induced magnetic field is negligible compared to the applied magnetic field. The stretching velocity is assumed to be $\bar{w} = w_w = a\bar{z}$ and the velocity upstream is assumed to be zero. In addition, a power law surface temperature and concentration of the form $T = T_w = T_\infty + A\bar{z}^p$ and $C = C_w = C_\infty + B\bar{z}^q$ is assumed. The physical properties of the fluid are assumed to be isotropic and constant except for the dynamic viscosity and thermal conductivity which are

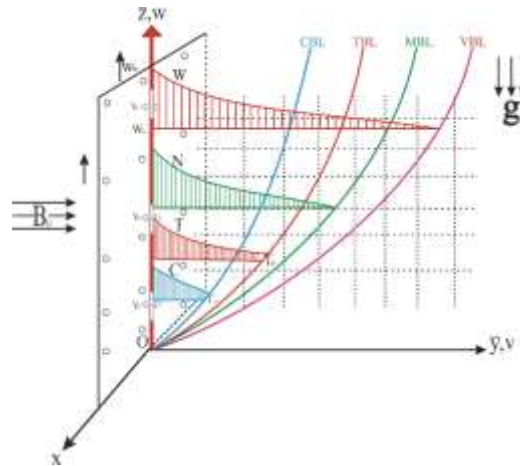


Fig. 1. Physical model and coordinate systems.

assumed to vary as a linear function of temperature and the density variation in the body force term of the momentum equation which is approximated by Boussinesq approximation. The fluid is assumed to be gray, absorbing and emitting but non-scattering medium and the radiative heat flux term in \bar{z} direction is considered negligible as compared to that in the \bar{y} direction.

Using the stated assumptions and the boundary layer approximations, the dimensional governing boundary layer equations of the fluid flow for mass, momentum, microrotation, energy and species concentration equations are given as:

$$\frac{\partial \bar{v}}{\partial \bar{y}} + \frac{\partial \bar{w}}{\partial \bar{z}} = 0, \quad (2.1)$$

$$\begin{aligned} \bar{v} \frac{\partial \bar{w}}{\partial \bar{y}} + \bar{w} \frac{\partial \bar{w}}{\partial \bar{z}} = & \frac{\mu}{\rho} \frac{\partial^2 \bar{w}}{\partial \bar{y}^2} + \frac{1}{\rho} \frac{\partial \mu}{\partial T} \frac{\partial T}{\partial \bar{y}} \frac{\partial \bar{w}}{\partial \bar{y}} + \frac{\kappa}{\rho} \frac{\partial^2 \bar{w}}{\partial \bar{y}^2} + \frac{\kappa}{\rho} \frac{\partial \bar{N}}{\partial \bar{y}} + g\beta_T (T - T_\infty) + \\ & g\beta_c (C - C_\infty) - \frac{\nu}{K_p} \bar{w} - \frac{F}{K_p} \bar{w}^2 - \frac{\sigma B_0^2}{\rho} \bar{w}, \end{aligned} \quad (2.2)$$

$$\bar{v} \frac{\partial \bar{N}}{\partial \bar{y}} + \bar{w} \frac{\partial \bar{N}}{\partial \bar{z}} = \frac{\gamma}{\rho j} \frac{\partial^2 \bar{N}}{\partial \bar{y}^2} - \frac{\kappa}{\rho j} \left(2\bar{N} + \frac{\partial \bar{w}}{\partial \bar{y}} \right), \quad (2.3)$$

$$\bar{v} \frac{\partial T}{\partial \bar{y}} + \bar{w} \frac{\partial T}{\partial \bar{z}} = \frac{1}{\rho C_p} \frac{\partial}{\partial \bar{y}} \left(k(T) \frac{\partial T}{\partial \bar{y}} \right) + \frac{\mu(T) + \kappa}{\rho C_p} \left(\frac{\partial \bar{w}}{\partial \bar{y}} \right)^2 - \frac{1}{\rho C_p} \frac{\partial q_r}{\partial \bar{y}} + \frac{D_m K_T}{C_s C_p} \frac{\partial^2 C}{\partial \bar{y}^2} + \frac{q'''}{\rho c_p}, \quad (2.4)$$

$$\bar{v} \frac{\partial C}{\partial \bar{y}} + \bar{w} \frac{\partial C}{\partial \bar{z}} = D \frac{\partial^2 C}{\partial \bar{y}^2} + \frac{D_m k_T}{T_m} \frac{\partial^2 T}{\partial \bar{y}^2} - k_r (C - C_\infty), \quad (2.5)$$

subject to boundary conditions

$$\begin{aligned} \bar{y} = 0 : \bar{w} = w_w = a\bar{z}, \bar{v} = v_{w(z)}, \bar{N} = -m \frac{\partial \bar{w}}{\partial \bar{y}}, T = T_w + A\bar{z}^p, C = C_w + B\bar{z}^q \\ \bar{y} \rightarrow \infty : \bar{w} \rightarrow 0, \bar{N} \rightarrow 0, T \rightarrow T_\infty, C \rightarrow C_\infty. \end{aligned} \quad (2.6)$$

Here, $\mu, \nu, \rho, \kappa, A$ and B are dynamic viscosity, kinematic viscosity, fluid density, vortex viscosity, A and B are constants.

Similarly, $T, C, N, k, g, B_o, \beta_T, \beta_T, F$ and K_p are the fluid temperature, fluid concentration, component of microrotation component, thermal conductivity, acceleration due to gravity, magnetic field intensity, coefficient of thermal expansion, coefficient of concentration expansion, Forchheimer constant and permeability of the porous medium.

Others are: $k_r, \sigma, C_p, p, q, T_w, C_w, T_\infty, C_\infty, D, c_s, K_T$ and q_r represent rate of chemical reaction, electrical conductivity, specific heat at constant pressure, wall temperature exponent, concentration exponent, fluid temperature of the stretching plate, free stream temperature, plate concentration and free steam concentration, molecular diffusivity, concentration susceptibility, thermal diffusion ratio and radiative heat flux respectively.

Also, m is a surface boundary parameter with $0 \leq m \leq 1$. The case when $m = 0$ corresponds to $N = 0$, this represents no-spin condition i.e. strong concentration such that the micro-particles close to the wall are unable to rotate. The case $m = \frac{1}{2}$, indicates weak concentration of micro-particles and the vanishing of anti-symmetric part of the stress tensor and the case $m = 1$ represents turbulent boundary layer flows (see Peddieson & McNitt [6]; Ahmadi, [4]; Jena and Mathur, [26]).

Also,

$$q''' = \frac{k w_w}{\bar{z} \nu} [A_1 (T_w - T_\infty) f' + B_1 (T - T_\infty)] \quad (2.7)$$

is the non-uniform heat source/sink (Pal and Chatterjee, 2010).

Here, A_1 and B_1 are coefficients of space and temperature dependent heat source/sink respectively. The case $A_1 > 0$ and $B_1 > 0$ corresponds to internal heat generation while $A_1 < 0$ and $B_1 < 0$ corresponds to internal heat absorption.

$\gamma = \left(\mu + \frac{\kappa}{2} \right) j$, is the spin gradient viscosity which denotes the relationship between the

coefficients of viscosity and micro-inertia, $j = \frac{V}{a}$, is the micro-inertia per unit mass. This assumption has been invoked to allow the field of eqns.(2.1 – 2.5) to predict the correct behaviour in the limiting case when the microstructure effects becomes negligible and the total spin N reduces to the angular velocity (Ahmadi, [4]). All the material constants $\mu, \kappa, \gamma, \nu, j$ are non-negative.

Furthermore, the temperature dependent viscosity and thermal conductivity are respectively given as (Mukhopadhyay *et al.*, [27]; Bhattacharyya *et al.*, [28])

$$\mu = \mu_{\infty} [b + c(T_w - T)] \tag{2.8}$$

$$k = k_{\infty} [1 + d(T - T_{\infty})] \tag{2.9}$$

Where μ_{∞} and k_{∞} are respectively the constant value of the coefficient of viscosity and thermal conductivity in the free stream, b , c and d are constants with $c > 0$ and d depends on the nature of the fluid. For fluids such as air and liquids as water, $d > 0$ while $d < 0$ for fluids such as lubricating oils.

Using Rosseland approximation,

$$q_r = - \frac{4\sigma^{\Sigma} \partial T^4}{3\alpha^{\Sigma} \partial y} \tag{2.10}$$

is the radiative heat flux (Brewster, [29]; Akinbobola and Okoya, [30]).

Assuming that there exists sufficiently small temperature difference within the flow such that T^4 can be expressed as a linear combination of the temperature. Expanding T^4 in Taylor series about T_{∞} to get

$$T^4 = T_{\infty}^4 + 4T_{\infty}^3(T - T_{\infty}) + 6T_{\infty}^2(T - T_{\infty})^2 + \dots, \tag{2.11}$$

neglecting higher order terms in eqn. (2.11) gives

$$T^4 \approx 4T_{\infty}^3 T - 3T_{\infty}^4, \tag{2.12}$$

substituting eqn. (2.12) in eqn.(10) to obtain

$$q_r = - \frac{16\sigma^{\Sigma} T_{\infty}^3 \partial T}{3\alpha^{\Sigma} \partial y}, \tag{2.13}$$

and differentiating eqn. (2.13) w. r. t. y gives

$$\frac{\partial q_r}{\partial y} = - \frac{16\sigma^{\Sigma} T_{\infty}^3 \partial T^2}{3\alpha^{\Sigma} \partial y^2}. \tag{2.14}$$

3 Non-dimensional form of the Governing Equations and Transformation to ODEs

Introducing the following dimensionless quantities

$$z = \frac{\bar{z}}{L}, y = \frac{\bar{y}\sqrt{Re}}{L}, w = \frac{\bar{w}}{w_w}, v = \frac{\bar{v}\sqrt{Re}}{w_w}, N = \frac{\bar{N}L}{w_w\sqrt{Re}} \quad (3.1)$$

$$\theta = \frac{T - T_\infty}{T_w - T_\infty}, \phi = \frac{C - C_\infty}{C_w - C_\infty}, Re = \frac{w_w L}{\nu}$$

Similarly, the stream function $\psi(y, z)$ is introduced as:

$$w = \frac{\partial \psi}{\partial y}, v = -\frac{\partial \psi}{\partial z}. \quad (3.2)$$

Using the stream function (3.2), the continuity equation (1) is automatically satisfied. Substituting (2.15) and (2.16) into (2.1 - 2.9) gives

$$\frac{\partial \psi}{\partial y} \frac{\partial^2 \psi}{\partial z \partial y} - \frac{\partial \psi}{\partial z} \frac{\partial^2 \psi}{\partial y^2} = (b + \xi(1 - \theta) + K) \frac{\partial^3 \psi}{\partial y^3} - \xi \frac{\partial \theta}{\partial y} \frac{\partial^2 \psi}{\partial y^2} + K \frac{\partial N}{\partial y} + Gr\theta +$$

$$Gc\phi - Da(b + \xi(1 - \theta)) \frac{\partial \psi}{\partial y} - Fs \left(\frac{\partial \psi}{\partial y} \right)^2 - M \frac{\partial \psi}{\partial y}, \quad (3.3)$$

$$\frac{\partial \psi}{\partial y} \frac{\partial N}{\partial z} - \frac{\partial \psi}{\partial z} \frac{\partial N}{\partial y} = \lambda \frac{\partial^2 N}{\partial y^2} - I \left(2N + \frac{\partial^2 \psi}{\partial y^2} \right), \quad (3.4)$$

$$\frac{\partial \psi}{\partial y} \left(p \frac{\theta}{z} + \frac{\partial \theta}{\partial z} \right) - \frac{\partial \psi}{\partial z} \frac{\partial \theta}{\partial y} = \frac{1}{Pr} \left(1 + h(\theta) + \frac{4}{3} R \right) \frac{\partial^2 \theta}{\partial y^2} + h \left(\frac{\partial \theta}{\partial y} \right)^2 + Du \frac{\partial^2 \phi}{\partial y^2} +$$

$$Ec(1 + \xi(1 - \theta) + K) \left(\frac{\partial^2 \psi}{\partial y^2} \right)^2 + \frac{1}{Pr} (1 + h\theta) \left(A_1 \frac{\partial \psi}{\partial y} + B_1 \theta \right), \quad (3.5)$$

$$\frac{\partial \psi}{\partial y} \left(q \frac{\phi}{z} + \frac{\partial \phi}{\partial z} \right) - \frac{\partial \psi}{\partial z} \frac{\partial \phi}{\partial y} = \frac{1}{Sc} \left(\frac{\partial^2 \phi}{\partial y^2} \right) + Sr \frac{\partial^2 \theta}{\partial y^2} - \gamma_1 \phi, \quad (3.6)$$

subject to the boundary conditions

$$\frac{\partial \psi}{\partial y} = z, \frac{\partial \psi}{\partial y} = fw, N = -m \frac{\partial^2 \psi}{\partial y^2}, \theta = z^p, \phi = z^q \text{ at } y = 0, \quad (3.7)$$

$$\frac{\partial \psi}{\partial y} \rightarrow 0, N \rightarrow 0, \theta \rightarrow 0, \phi \rightarrow 0 \text{ as } y \rightarrow \infty.$$

Where $K = \frac{\kappa}{\mu}$ is the material parameter, $Gr = \frac{g\beta_T(T_w - T_\infty)L}{w_w^2}$ is the local temperature

Grashof number, $Gc = \frac{g\beta_C(C_w - C_\infty)L}{w_w^2}$ is the local species concentration Grashof number, $Pr =$

$\frac{\mu C_p}{k}$ is the Prandtl number, $Sc = \frac{\nu}{Dm}$ is the Schmidt number, $fw = -\frac{v_w \sqrt{Re}}{w_w}$ is the

suction/injection parameter, $Ec = \frac{w_w^2}{Cp(T_w - T_\infty)}$ is the Eckert number, $Da = \frac{\nu L}{w_w}$ is the Darcy

number, $Fs = \frac{LF}{K_p}$ is the Forchheimer number, $Du = \frac{DmK_T(C_w - C_\infty)L}{CsCp\nu(T_w - T_\infty)}$ is the Dufour number,

$Sr = \frac{DmK_T(T_w - T_\infty)L}{T_m\nu(C_w - C_\infty)}$ is the Soret number, $R = \frac{4\sigma\Sigma T_\infty^3}{\alpha\Sigma k_\infty}$ is the radiation parameter, $I = \frac{\kappa L}{w_w\rho j}$

is the vortex viscosity parameter, $M = \frac{\sigma B_o^2 L}{w_w\rho}$ is the magnetic field parameter, $\lambda = \frac{\gamma}{\nu\rho j}$

microrotation density parameter, $\gamma_1 = \frac{k_r L}{w_w}$ is the homogeneous chemical reaction parameter.

Also, $h = d(T_w - T_\infty)$ is the thermal conductivity parameter. The range of variation of h can be as follows: for air $0 \leq h \leq 6$, for water $0 \leq h \leq 0.12$ and for lubricating oils $-0.1 \leq h \leq 0$ (Seddek and Abdelmeguid, [31]).

Introducing simplified form of Lie-group transformations namely, the scaling group of transformations to equations (3.3)-(3.7) is equivalent to determining the invariant solutions of these equations under a continuous one-parameter group (Mukhopadhyay, [22]; Dada and Salawu, [32]). One of the methods is to search for a transformation group from an elementary set of one-parameter scaling group of transformations, given as Γ

$$\begin{aligned} \Gamma : z^* &= ze^{\alpha_1}, y^* = ye^{\alpha_2}, \psi^* = \psi e^{\alpha_3}, \theta^* = \theta e^{\alpha_4}, \phi^* = \phi e^{\alpha_5}, \\ N^* &= Ne^{\alpha_6}, w^* = we^{\alpha_7}, v^* = ve^{\alpha_8}. \end{aligned} \quad (3.8)$$

Here, $\alpha_1, \alpha_2, \alpha_3, \alpha_4, \alpha_5, \alpha_6, \alpha_7$, and α_8 are transformation parameters which are arbitrary real numbers not all zero simultaneously and ε is a small parameters. Equation (3.8) is considered as a point-transformation which transforms coordinate $(z, y, \psi, \theta, \phi, N, w, v)$ to the coordinates $(z^*, y^*, \psi^*, \theta^*, \phi^*, N^*, w^*, v^*)$.

The task is to establish relationships among the exponents α_i 's such that equations (3.3)-(3.7) will remain invariant under the point transformations. Substituting transformation (3.8) into Equations (3.3)-(3.7) and applying invariant conditions yields

$$\alpha_1 = \alpha_3 = \alpha_4 = \alpha_5 = \alpha_6 = \alpha_7, \alpha_2 = \alpha_8 = 0, \alpha_3 = \frac{1}{2}\alpha_1, \alpha_4 = \frac{1}{2}\alpha_1. \quad (3.9)$$

Hence, the set of transformations Γ reduces to one parameter group of transformations as

$$z^* = ze^{\alpha_1}, y^* = y, \psi^* = \psi e^{\alpha_1}, \theta^* = \theta e^{\alpha_1}, \phi^* = \phi e^{\alpha_1}, N^* = Ne^{\alpha_1}, w^* = \theta e^{\alpha_1}, v^* = v. \quad (3.10)$$

Finding the absolute invariant, the similarity transformations becomes:

$$\eta = y, \psi = z^* f(\eta), N^* = z^* g(\eta), \theta^* = z^* \theta(\eta), \phi^* = z^* \phi(\eta). \quad (3.11)$$

On substituting (3.11) into equations (3.3) - (3.7), the results yield the system of non-linear ordinary differential equations as:

$$\begin{aligned} (b + \xi(1 - \theta) + K)f'''' - \xi\theta f''' + ff'' + Kg' + Gr\theta + Gc\phi - \\ (Da(b + \xi(1 - \theta)) + M)f' - (Fs + 1)f'^2 = 0, \end{aligned} \quad (3.12)$$

$$\lambda g'' + fg' - fg - I(2g + f'') = 0, \quad (3.13)$$

$$\begin{aligned} \left(1 + h\theta + \frac{4}{3}R\right)\theta'' + h\theta'^2 - PrEc(b + \xi(1 - \theta) + K)f''^2 + PrDu\phi'' + \\ Pr(f\theta' - p\mathcal{G}f') + (1 + h\theta)(A_1f' + B_1\theta) = 0, \end{aligned} \quad (3.14)$$

$$\phi'' + ScSr\theta'' + Sc(f\phi' - q\phi') - Sc\gamma_1\phi = 0, \quad (3.15)$$

subject to boundary conditions

$$\begin{aligned} \eta = 0 : f' = 1, f = fw, g = -mf'', \theta = 1, \phi = 1, \\ \eta \rightarrow \infty : f' \rightarrow 0, g \rightarrow 0, \theta \rightarrow 0, \phi \rightarrow 0. \end{aligned} \quad (3.16)$$

Where, primes denote differentiation with respect to η .

The Physical Quantities of Interest

The physical quantities of engineering interest are the skin friction coefficient Cf_z , couple stress Cs , the local Nusselt number Nu , local Sherwood number Sh . These are respectively defined as (Mohammed and Ado-Dahab, [16]).

$$Cf_z = \frac{\tau_w}{\rho w_w}, \quad Cs = \frac{\bar{z}M_w}{\mu j w_w}, \quad Nu = \frac{\bar{z}q_w}{k_\infty(T_w - T_\infty)}, \quad Sh = \frac{\bar{z}q_m}{Dm(C_w - C_\infty)}. \quad (3.17)$$

Here, τ_w is the wall shear stress, M_w is the wall couple stress, q_w is the heat flux and q_m is the mass flux. These are respectively defined as:

$$\begin{aligned} \tau_w = \left[(\mu + \kappa) \frac{\partial \bar{w}}{\partial \bar{y}} + \kappa \bar{N} \right]_{\bar{y}=0}, \quad M_w = \left(\gamma \frac{\partial \bar{N}}{\partial \bar{y}} \right)_{\bar{y}=0}, \quad q_w = -k \left[\left(1 + \frac{4R}{3} \right) \frac{\partial T}{\partial \bar{y}} \right]_{\bar{y}=0}, \\ q_m = -Dm \left[\frac{\partial C}{\partial \bar{y}} \right]_{\bar{y}=0}. \end{aligned} \quad (3.18)$$

4 Method of solution: Weighted Residuals Method

Weighted residuals method works by seeking is to seek for an approximate solution, in form of a polynomial to the differential equation of the form

$$H[w(z)] = f(z) \text{ in the domain } Y, \quad B_\mu[w] = \gamma_\mu \text{ on } \partial Y, \quad (4.1)$$

where $H[w]$ denotes a differential operator linear or non-linear involving spatial derivatives of dependent variables w , f is known function of position, $B_\mu[w]$ represents the approximate number of boundary conditions and Y is the domain with boundary ∂Y .

Assuming a polynomial known as trial function with unknown coefficients or parameters to be determined later for equations (3.12-3.15)

$$f(\eta) = \sum_{i=0}^n a_i \eta^i, \quad g(\eta) = \sum_{i=0}^n b_i \eta^i, \quad \theta(\eta) = \sum_{i=0}^n c_i \eta^i, \quad \phi(\eta) = \sum_{i=0}^n d_i \eta^i. \quad (4.2)$$

Imposing the boundary conditions (3.16) on the trial functions (4.2). Also substituting equation (4.2) into equations (3.12 -3.15) to obtain the residual equations as:

$$\begin{aligned} fr = & (b + \xi(-\eta^5 c_5 - \eta^4 c_4 - \eta^3 c_3 - \eta^2 c_2 - \eta c_1 - c_0 + 1) + K)(60\eta^2 a_5 + \\ & 24\eta a_4 + 6a_3) - \xi(5\eta^4 c_5 + 4\eta^3 c_4 + 3\eta^2 c_3 + 2\eta c_2 + c_1)(20\eta^3 a_5 + 12\eta^2 a_4 + \\ & 6\eta a_3 + 2a_2) + \dots, \end{aligned} \quad (4.3)$$

$$\begin{aligned} gr = & \lambda(20\eta^3 b_5 + 12\eta^2 b_4 + 6\eta b_3 + 2b_2) + (\eta^5 a_5 + \eta^4 a_4 + \eta^3 a_3 + \eta^2 a_2 + \eta a_1 + \\ & a_0)(5\eta^4 b_5 + 4\eta^3 b_4 + 3\eta^2 b_3 + 2\eta b_2 + b_1) - \end{aligned} \quad (4.4)$$

$$\theta^r = \left(1 + h(\eta^5 c_5 + \eta^4 c_4 + \eta^3 c_3 + \eta^2 c_2 + \eta c_1 + c_0) + 4/3R\right) (20\eta^3 c_5 + 12\eta^2 c_4 + 6\eta c_3 + 2c_2) + h(5\eta^4 c_5 + 4\eta^3 c_4 + 3\eta^2 c_3 + 2\eta c_2 + c_1)^2 + PrEc(b + K + (-\eta^5 c_5 - \eta^4 c_4 - \eta^3 c_3 - \eta^2 c_2 - \eta c_1 - c_0 + 1)\xi) \quad (4.5)$$

$$\phi^r = 20\eta^3 d_5 + 12\eta^2 d_4 + 6\eta d_3 + 2d_2 + ScSr(20\eta^3 c_5 + 12\eta^2 c_4 + 6\eta c_3 + 2c_2) + \quad (4.6)$$

where, f^r , g^r , θ^r and ϕ^r represents the residual for the momentum, microrotation, energy and concentration equations respectively.

The residuals equations (35-38) are forced to zero at a number of selected points within the domain at a regular interval and symmetry consideration. The values of the governing flow parameters are also substituted into the residuals equations.

The resulting equations are then solved to obtain the values of the unknown parameters which are then substituted into (4.2) to obtain the velocity $f(\eta)$, temperature $\theta(\eta)$, microrotation $g(\eta)$ and concentration $\phi(\eta)$. This procedure is repeated for four different values each for the embedded physical parameters $M, K, Gr, Gc, \xi, h, Pr, Ec, Sr, Sc, R, Du, Da, Fs, \gamma_1, A_1, B_1, I, \lambda$ and fw . The computational results are obtained and compared well with fourth order Runge-Kutta method as shown in Table 1.

		$f''(0)$		$g'(0)$		$-\theta'(0)$		$-\phi'(0)$	
PP	Values	WRM	RK	WRM	RK	WRM	RK	WRM	RK
K	0.0	1.718412	1.723056	2.183574	2.185908	0.675616	0.674722	0.884279	0.885054
	1.0	1.126107	1.130291	1.441585	1.443577	0.658300	0.657592	0.877185	0.877847
	2.5	0.742326	0.746419	0.971700	0.973528	0.642828	0.642235	0.869633	0.870351
M	0.0	1.207297	1.211597	1.531046	1.533090	0.675696	0.675152	0.883442	0.884178
	1.0	0.857335	0.861449	1.142036	1.144039	0.533804	0.532300	0.859960	0.860470
	2.5	0.355370	0.359571	0.599722	0.601804	0.430251	0.427495	0.820635	0.820835
Gr	4.0	0.635228	0.641268	0.883322	0.886272	0.587104	0.586154	0.821261	0.822212
	5.5	1.086073	1.091927	1.382347	1.385346	0.602791	0.602066	0.853854	0.854867
	6.5	1.377550	1.383239	1.712204	1.715193	0.607812	0.607183	0.873790	0.874807
Gc	4.0	1.164361	1.168653	1.478715	1.480766	0.598837	0.598014	0.883567	0.884290
	5.5	1.515117	1.518776	1.887343	1.889051	0.663762	0.663060	0.901510	0.902102
	6.5	1.767228	1.770583	2.181204	2.182749	0.664131	0.663443	0.916383	0.916929
ξ	0.0	1.4075144	1.419027	1.611992	1.621520	0.400097	0.394772	0.917168	0.919440
	1.5	1.2258581	1.240265	1.532391	1.543496	0.368647	0.362446	0.897862	0.900352
	3.0	1.1178133	1.136146	1.421850	1.437156	0.357776	0.351022	0.885396	0.888246
h	0.0	0.977015	0.982033	1.286872	1.289290	1.040160	1.039052	0.853483	0.854388
	0.75	1.091327	1.095720	1.406018	1.408113	0.729567	0.728791	0.871801	0.872523
	1.5	1.192344	1.196119	1.508416	1.510212	0.541395	0.540790	0.887415	0.887963
Pr	0.72	1.126107	1.130291	1.441585	1.443577	0.658300	0.657592	0.877185	0.877847
	1.0	0.984367	0.988116	1.302759	1.304381	0.886908	0.886654	0.853620	0.854075
	1.5	0.826048	0.829614	1.141669	1.143070	1.224923	1.225006	0.828212	0.828538

Table 1: The values of $f''(0)$, $g'(0)$, $-\theta'(0)$ and $\phi'(0)$ for variation in K, M, Gr, Gc, ξ, h and Pr for both WRM and RK (PP-Physical Parameters)

5 Results and Discussion

To have a clear insight into the behaviour of the fluid flow, a computational analysis has been carried out for the velocity, temperature, concentration and microrotation. The default values adopted for computation are: $K = fw = I = \lambda = 1$, $Gr = Gc = 4$, $R = Du = 0.5$, $A_1 = B_1 = M = Ec = 0.2$, $Da = 0.5 = Fs = m$, $\gamma_1 = 0.01$, $Sr = 0.1$, $Pr = 0.72$, and $Sc = 0.22$. Hence, the graphs correspond to these values unless otherwise indicated on the graph.

Table 1 shows the computational values of the skin friction coefficient $f''(0)$, the wall couple stress $g'(0)$, the local Nusselt number $-\theta'(0)$ and the local Sherwood number $-\phi'(0)$ for selected physical parameters. The obtained values by Weighted residuals method (WRM) are also validated by comparison with fourth order Runge-Kutta technique alongside shooting method. The presentation shows a perfect agreement between the two methods. From this table, the material parameter K , the magnetic parameter M , the viscosity parameter ξ and the Prandtl parameter Pr have a decreasing influence on the skin friction coefficient. In addition, the increase in the viscosity ξ and material K parameters reduce the wall couple stress, rate of heat and mass transfers as well.

The skin friction coefficient increases in value for a rise in thermal conductivity parameter h , thermal and solutal Grashof numbers (Gr and Gc). Also Prandtl Pr and thermal Grashof Gr parameters cause an increase the local Nusselt number while a rise in the solutal Grashof parameter Gc produces an increase in the local Sherwood number..

Figs. 2-3 depict the influence of magnetic field parameter M on the velocity and temperature profiles. As shown, the velocity decreases with an increase in the value of the magnetic field parameter M . This response is due to the imposition of the transverse magnetic field in an electrically conducting fluid which induces a resistive force known as Lorentz force acting against the fluid motion and slows it down. However, due to the resistance to the fluid motion imposed by the Lorentz force due to magnetic field, the temperature rises with increasing values of M as displayed in Fig. 3.

Fig. 4 displays the impact of the material parameter K on the velocity distribution. It is evident that the velocity profiles near the plate decrease as K increases due to the reduction in the boundary layer thickness. Further from the plate, the profiles overlap due to the dominance of kinematic viscosity, and then decrease with an increase in K with the velocity of non-Newtonian micropolar fluid higher than that of Newtonian fluid (i.e. $K = 0$).

Figs. 5 and 6 describe the combined influence of increasing Dufour Du while decreasing Soret Sr on the velocity profiles. The values of Sr and Du are selected in such a way that their products are constant according to their definition, assuming that the mean fluid temperature T_m is kept constant. Evidently, both the velocity and temperature rise with increasing Dufour Du (while decreasing Soret) due to increase in momentum and thermal boundary layer thickness.

Figs. 7-10 describe the influence the suction/injection parameter fw on the velocity, temperature, concentration and microrotation profiles. A decrease in the velocity, temperature and microrotation profiles is observed with an increase in the suction parameter (fw). The thinning effects of ($fw > 0$) on these profiles can be attributed to the fact that the heated fluid is being pushed towards the plate such that the buoyancy force acted to retard the fluid as a result of high influence of viscosity. In addition, the fluid is brought closer to the surface such that it reduces the thermal and solutal boundary layer thickness. However, the imposition of wall

fluid injection $f_w < 0$ produces the opposite effect as it enhances velocity distribution within the boundary layer. The microrotation profiles rises near the plate with increase in f_w whereas away from the plate the profiles overlap and then fall. Negative values indicate reverse rotation of micro-elements.

Fig. 11 illustrates the temperature profiles with η for different values of Prandtl number

Pr . Clearly, an increase in the value of the Prandtl number Pr produces a dampen effect on the temperature profiles. Physically, Prandtl number expresses the ratio of momentum diffusivity to thermal diffusivity and it controls the relative thickness of the momentum and thermal boundary layers. Hence, increasing Prandtl number Pr implies reduction in thermal boundary layer thickness which in turn lowers the average temperature within the boundary layer. Thus, Prandtl parameter Pr can therefore be applied to enhance the rate of cooling as fluids with moderate Prandtl number Pr creates higher conductivities and at such heat diffuses quickly away from the heated vertical plate than for higher values of Prandtl number Pr .

Figs. 12-15 portray the influences of space dependent heat source ($A_1 > 0$) and space dependent heat sink ($A_1 < 0$) on the dimensionless velocity and temperature profiles. Clearly, an increase in ($A_1 > 0$) enhances both the velocity and temperature distributions due to a rise in momentum and thermal boundary layer thickness as ($A_1 > 0$) increases. In addition, energy is generated by the imposition $A_1 > 0$ leading to an increase in the micropolar fluid temperature, thereby causing a rise in the temperature profiles. In consequence, the buoyancy force rises leading to a rise in the fluid motion in the presence of micro-elements. The trend is however reversed for the space dependent heat sink ($A_1 < 0$) as shown in Fig. 13 due to the thickening of momentum boundary layer thickness.

The influences of $A_1 > 0$ and $A_1 < 0$ on temperature profiles are displayed in Figs. 14 and 15. It is evident from from Fig. 14 that the thermal boundary layer thickness increases with a rise in the magnitude of ($A_1 > 0$), while it falls with an increase in $A_1 < 0$. Fig. 16 describes the effect of heat generation parameter $B_1 > 0$ on temperature profiles across the boundary layer. Observation shows that the presence of heat source $B_1 > 0$ enhances the fluid temperature and also causing the thermal boundary layer thickness to increase due to the fact that more energy is generated in the boundary layer leading to a rise in the micropolar fluid temperature.

Figs. 17-18 depict the impact of the homogeneous chemical reaction parameter γ_1 on the concentration distribution. It is shown that an increase in destructive chemical reaction parameter ($\gamma_1 > 0$) leads to a decrease in concentration of the micropolar fluid as displayed in Fig. 17 due to the reduction in the solutal boundary layer thickness. On the other hand, generative reaction ($\gamma_1 < 0$), produces a reverse trend as illustrated in Fig.18. In addition, the magnitude of destructive chemical reaction ($\gamma_1 > 0$) is lower than that of generative chemical reaction ($\gamma_1 < 0$) due to the fact that $\gamma_1 > 0$ occurs with much disturbances than $\gamma_1 < 0$, hence, molecular motion in the case of $\gamma_1 > 0$ is much greater which leads to an increase in mass transport phenomenon.

The influences of Darcy Da and Forchheimer Fs parameters on the velocity profiles are displayed in Figs. 19-20. It is observed that the velocity decreases for both Da and Fs parameters. Increase in the Darcy Da and Forchheimer parameters imply that the porous

medium is causing more resistance to the fluid flow, as a result of this, the flow velocity decreases.

The increase in thermal conductivity parameter h enhances both the fluid velocity and temperature due to increase in momentum and thermal boundary layer thickness as displayed in Figs. 21-22. Fig. 23 illustrates the effect of viscosity variation parameter ξ on the velocity profiles. Observation shows that velocity profiles decrease rapidly near the plate whereas, further from the plate as η increases the effect of ξ becomes negligible. This response is due to the growth in magnitude of ξ implying an increase in $(T_w - T)$ at a constant value c . In consequence, the time of interaction between neighbouring molecules and intermolecular forces between the fluid is reduced. This causes the fluid viscosity to increase leading to the reduction in the flow motion.

The effects of radiation parameter R on velocity and temperature distributions are displayed in Figs. 24 and 25. Both the dimensionless fluid velocity and temperature increase as the magnitude of radiation parameter R increases. By implication, radiation parameter R enhances both velocity and temperature distributions across the boundary layer. As the rate of radiative heat transfer to the fluid increases, the fluid temperature rises which in turn induces thermal buoyancy effect, leading to a rise in the fluid velocity. Hence, to have the cooling process at a faster rate R should be reduced

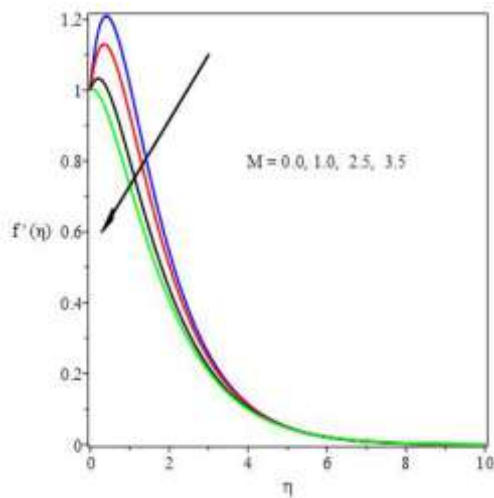


Fig. 2. Effect of M on velocity profiles

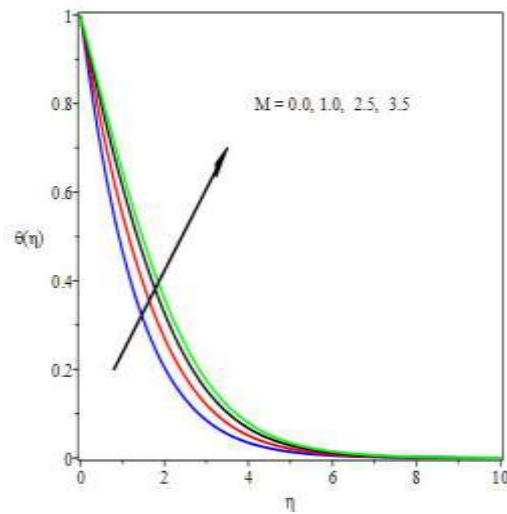


Fig. 3. Effect of M on temperature profiles

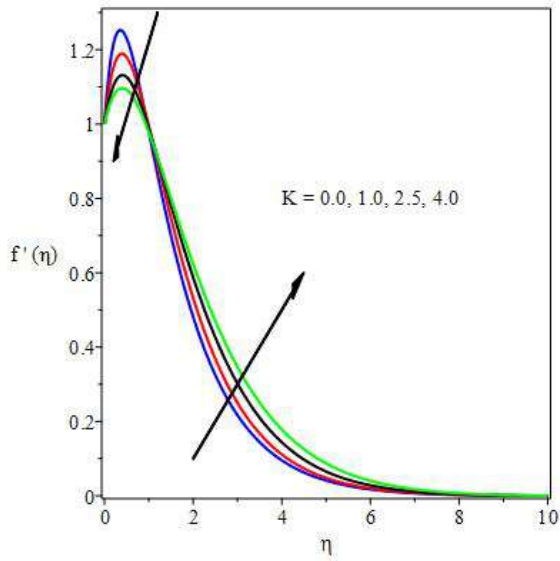


Fig. 4. Effect of K on velocity profiles 1

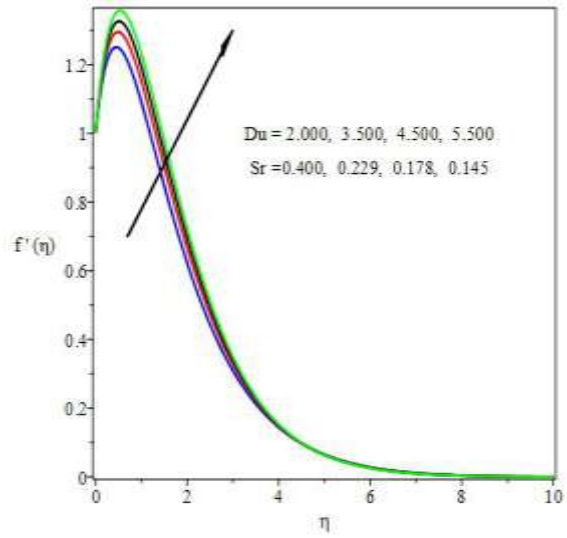


Fig. 5. Effect of Du & Sr on velocity prof 1

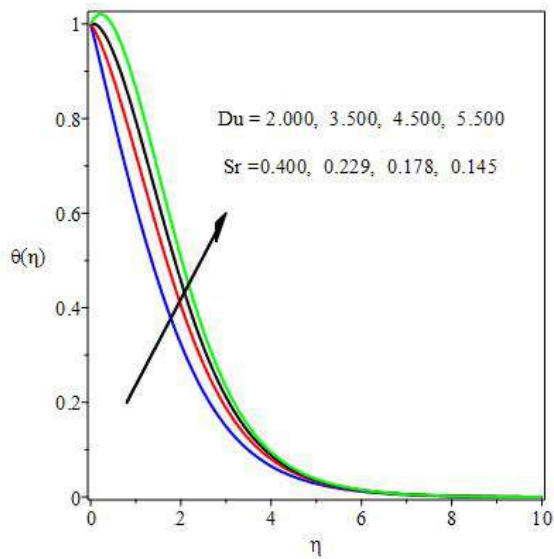


Fig. 6. Effect of Du & Sr on temperature p 1

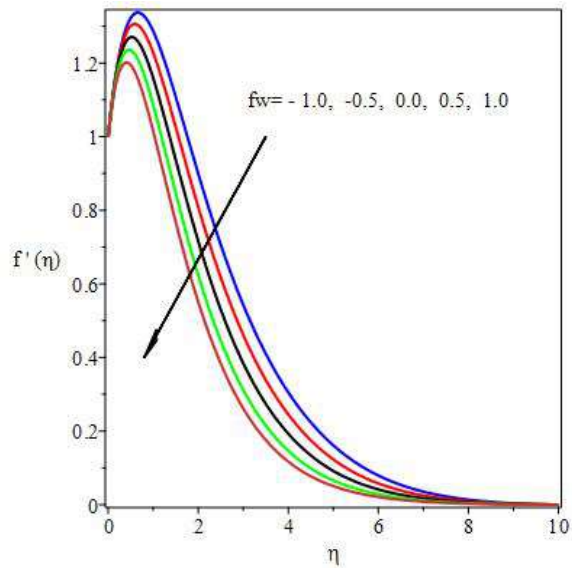


Fig. 7. Effect of fw on velocity profiles 1

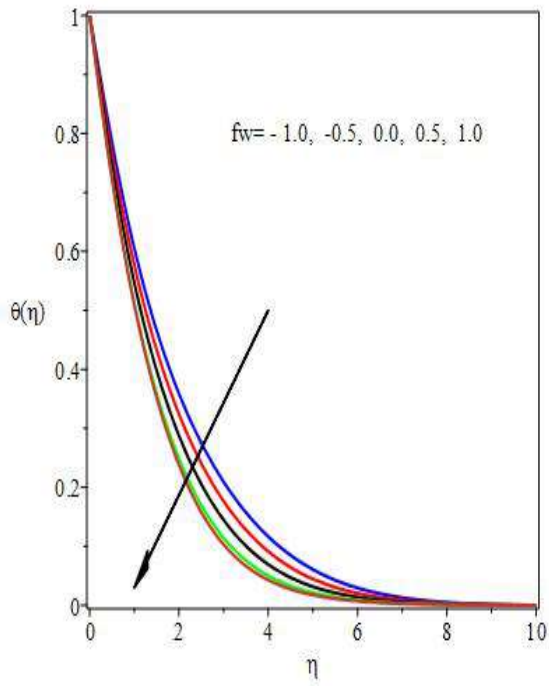


Fig. 8. Effect of f_w on temperature profiles profiles

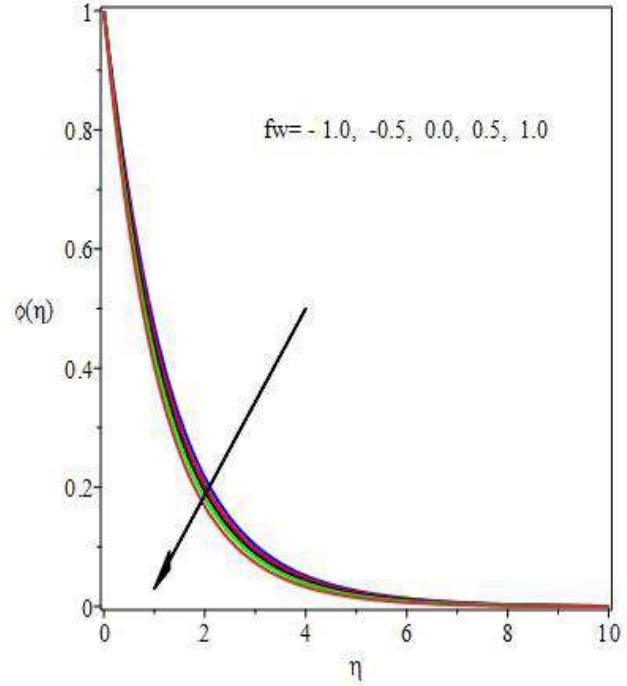


Fig. 9. Effect of f_w on concentration

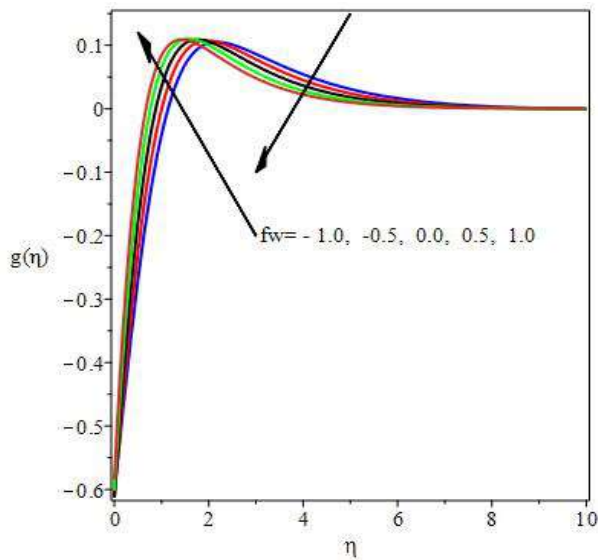


Fig.10. Effect of f_w on microrotation profiles

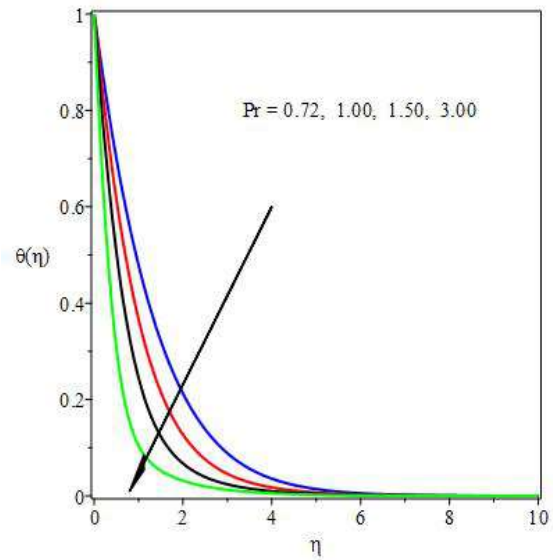


Fig.11. Effect of Pr on temperature profiles

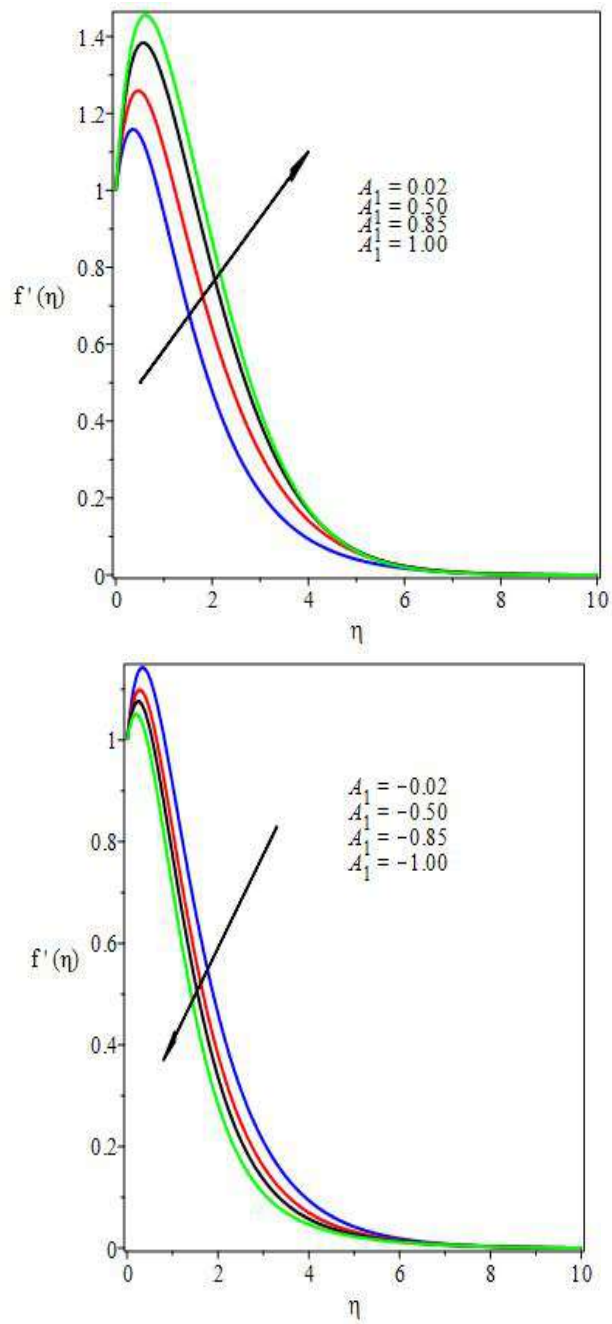


Fig. 12. Effect of $A_1 > 0$ velocity profiles **Fig. 13.** Effect of $A_1 < 0$ on velocity profiles

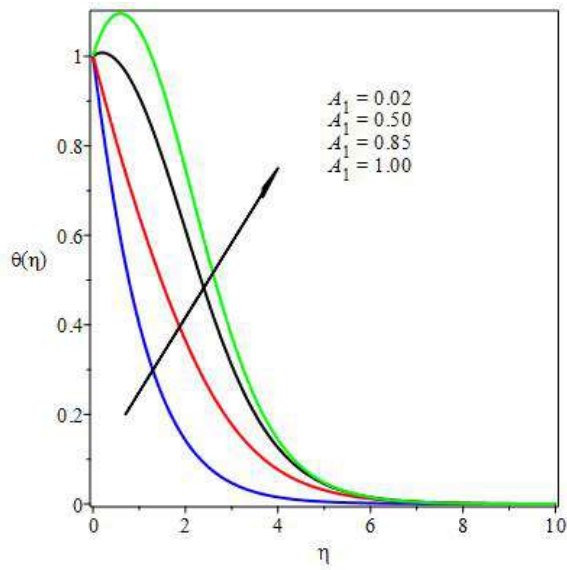


Fig. 14. Effect of $A_1 > 0$ on temperature profiles

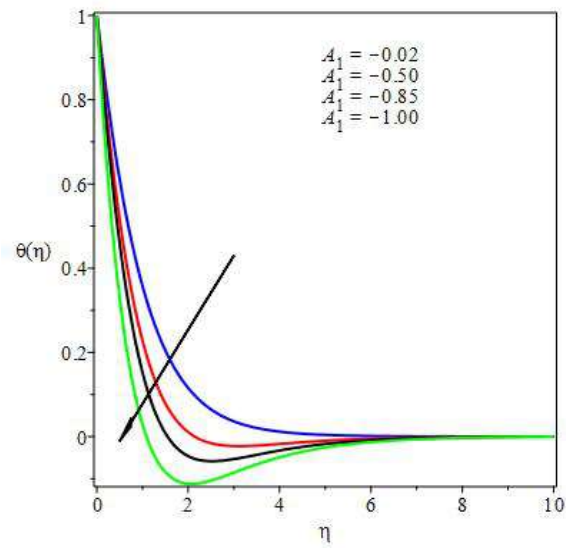


Fig. 15. Effect of $A_1 < 0$ on temperature profiles

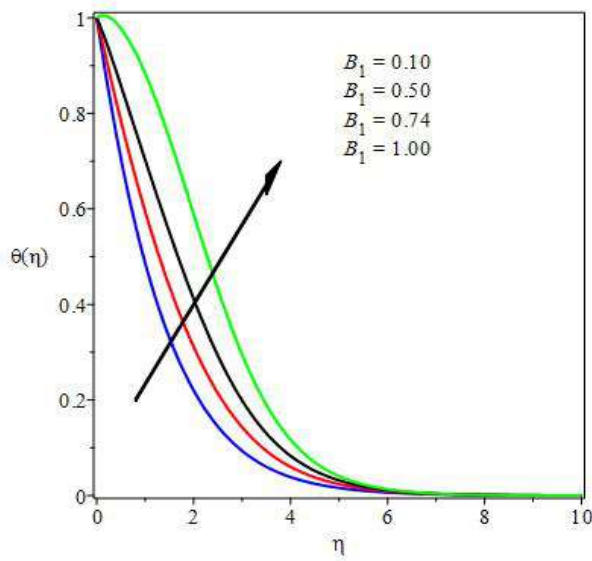


Fig. 16. Effect of $B_1 > 0$ on temperature profiles

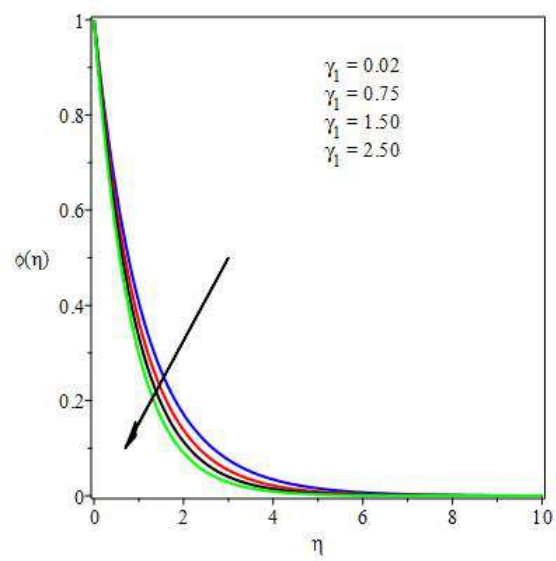


Fig. 17. Effect of $\gamma_1 > 0$ on concentration profiles

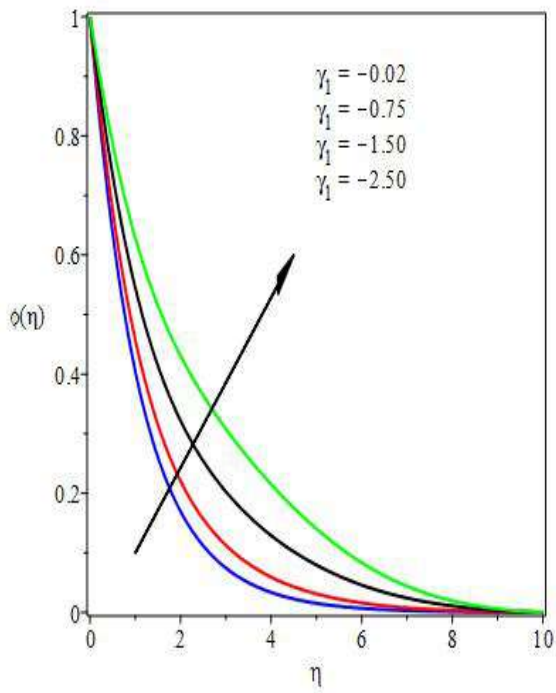


Fig. 18. Effect of $\gamma_1 < 0$ on concentration profiles

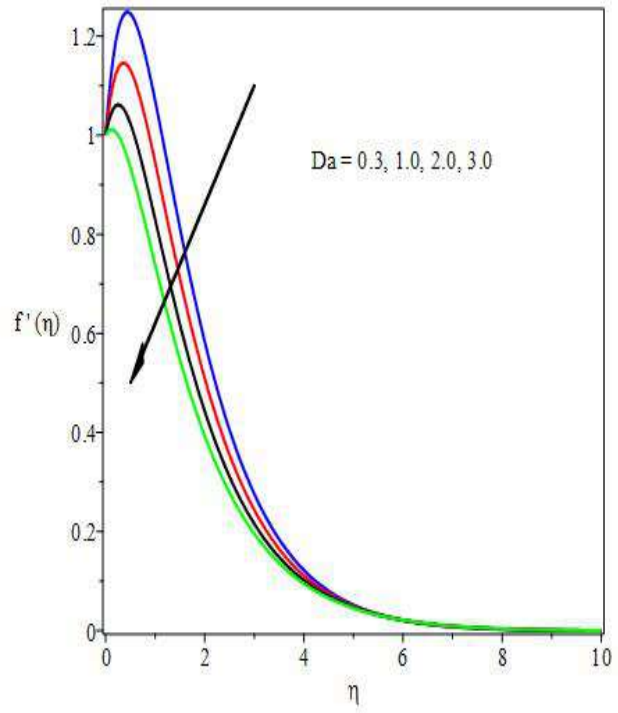


Fig. 19. Effect of Da on velocity profiles

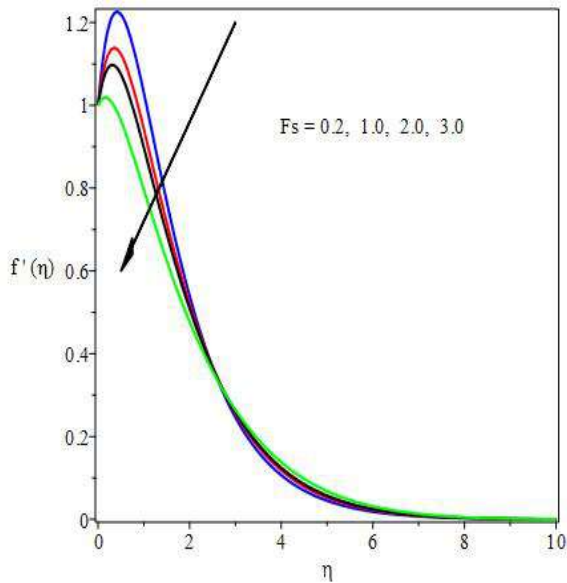


Fig. 20. Effect of Fs on velocity profiles

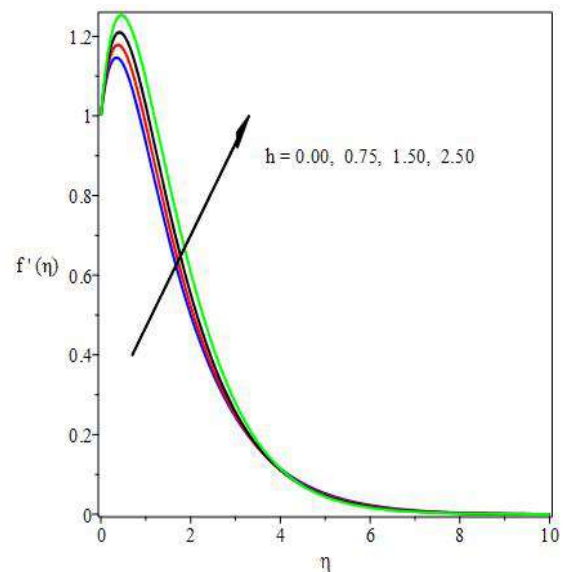


Fig. 21. Effect of h on velocity profiles

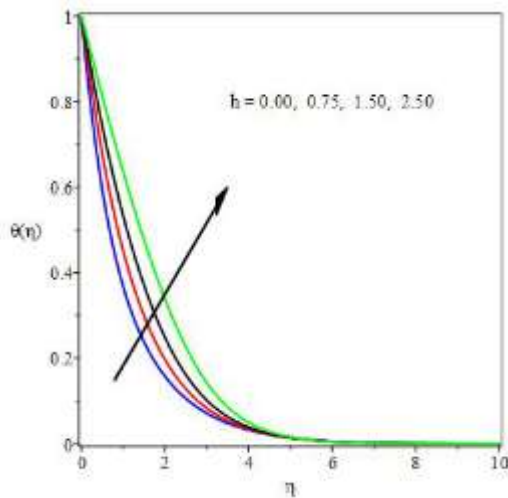


Fig. 22. Effect of h on temperature profiles

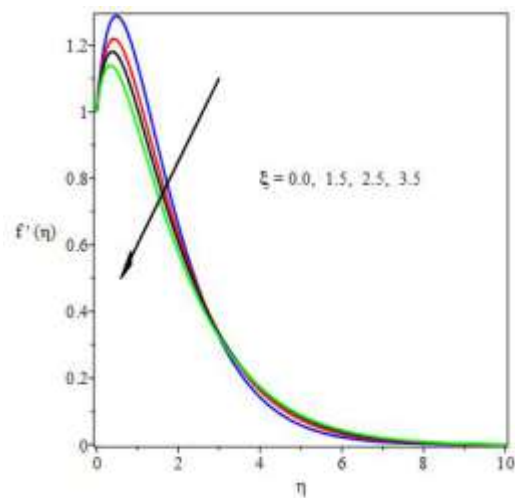


Fig. 23. Effect of ξ on velocity profiles

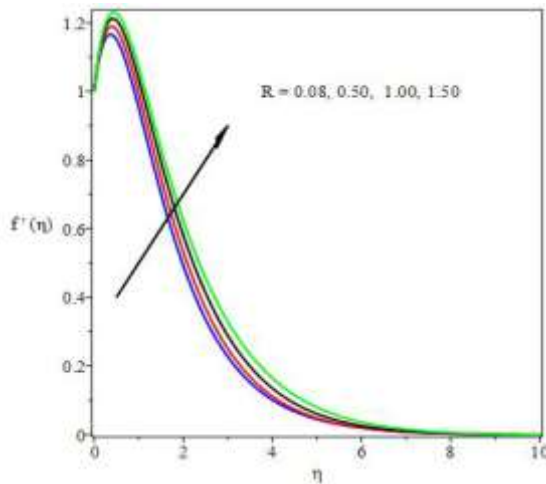


Fig. 24. Effect of R on velocity profiles

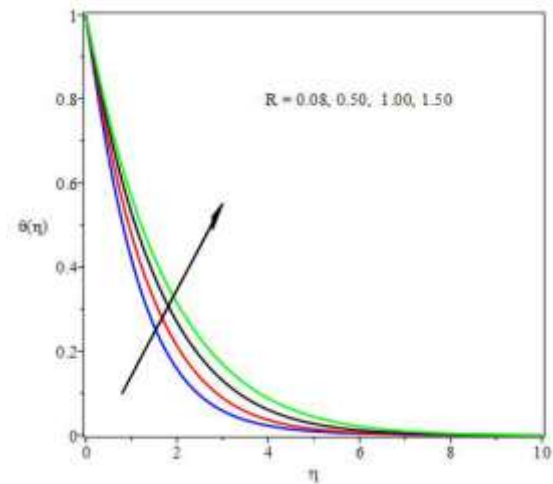


Fig. 25. Effect of R on temperature profiles

6 Conclusion

The present study is an investigation of heat and mass transfer of thermally radiating and chemically reacting MHD micropolar fluid flow past a permeable stretching sheet in a porous medium with Soret and Dufour effects and non-uniform heat source/sink. Lie-group scaling analysis was used to develop similarity variables which were in turn applied to transform the governing PDEs of the fluid flow into non-linear ODEs. The resulting equations were solved by Weighted residuals method via collocation technique. The results compared well with shooting method alongside with fourth order Runge-Kutta method. The influences of the emerging physical parameters on the dimensionless velocity, microrotation, temperature and species concentration profiles are graphically presented and discussed. Moreover, the effects of pertinent flow parameters on the skin friction $f''(0)$, wall couple stress $g'(0)$, Nusselt number $-\theta'(0)$ and the Sherwood number $-\phi'(0)$ are tabulated.

The following conclusions were drawn from this study:

- The material (micropolar) parameter K causes a decrease in the fluid velocity near the plate while increasing it further away from the plate.

- The influence of K is to decrease the skin friction coefficient $f''(0)$, heat transfer $\theta'(0)$ and wall couple stress $g'(0)$. Thus K can be useful in reducing drag along the plate.
- An increase in the magnetic parameter M reduces the fluid motion but enhances temperature distribution.
- Increasing Dufour number Du while decreasing Soret number Sr causes a rise in both the fluid velocity and Temperature while decreasing the concentration.
- Thermal Grashof number Gr and solutal Grashof number Gc increase the skin friction coefficient, wall couple stress, heat and mass transfer whereas viscosity parameter ξ deceases these quantities.
- Prandtl number Pr reduces the skin friction but enhances heat transfer rate while thermal conductivity parameter h enhances skin friction coefficient.
- An increase in destructive chemical reaction parameter ($\gamma_1 > 0$) causes a decrease in concentration while generative chemical reaction parameter ($\gamma_1 < 0$) enhances it.
- The influences of space dependent heat source $A_1 > 0$ and temperature dependent heat source $B_1 > 0$ is to increase both velocity and temperature distributions whereas $A_1 < 0$ dampens temperature.

Competing financial interests

The authors declare no competing financial interests”.

References

- [1] Eringen, A. C. Theory of micropolar fluids, *J. Math. Anal. Appl.*, 16, 1-18 (1966).
- [2] Eringen, A. C. Theory of thermo-microfluids, *Journal of Mathematical Analysis and Applications*, 38, 480-496 (1972).
- [3] Lukaszewicz, G. *Micropolar fluids: Theory and Applications* 1st Ed., Birkhauser, Boston (1999).
- [4] Ahmadi, G. Self-similar solution of incompressible micropolar boundary layer flow over a semi-infinite plate, *Int. J. Engng Sci*, 1, 639-646 (1976).
- [5] Hayat, T., Shehzad, S. A. & Qasim, M. Mixed convection flow of a micropolar fluid with radiation and chemical reaction, *Int J. Numer Meth*, 67, 1418-1436 (2011).
- [6] Peddieson, J & McNitt, R. P. Boundary layer theory for micropolar fluid, *Recent Adv. Eng. Sci.*, 5, 405 (1970).
- [7] Crane, L. J. Flow past a stretching plate, *Communications Breves*, 21, 645-647 (1970).
- [8] Gupta, P. S. & Gupta, A. S. Heat and mass transfer on a stretching sheet with suction or blowing, *Can. J. Chem. Eng.*, 55, 744-746 (1977).
- [9] Eldabe, N. T., Elshehawey, E. F., Elbarbary, M. E. & Elgazery, N. S. Chebyshev finite - difference method for MHD flow of a micropolar fluid past a stretching sheet with heat transfer, *Journal of Applied Mathematics and Computation*, 160, 437-450 (2003).
- [10] Elbashbeshy, E. M. A. & Bazid, M. A. A. Heat transfer in a porous medium over a stretching surface with internal heat generation and suction or injection *Applied Mathematics and Computation*, 158, (3), 15, 799-807 (2004).
- [11] Kumar, L. Finite element analysis of combined heat and mass transfer in hydromagnetic micropolar flow along a stretching sheet. *Comput Mater Sci*, 46, 841-848 (2009).
- [12] Hayat, T., Mustafa, M. & Obaidat, S. Soret and Dufour effects on the stagnation-point flow of a micropolar fluid toward a stretching sheet, *Journal of Fluid Engineering*, 133,

- 1-9 (2011).
- [13] Reddy, P. S. & Chamkha, A. J. Soret and Dufour on MHD heat and mass transfer flow of a micropolar fluid with thermophoresis particle deposition, *Journal of Naval Architecture and Marine Engineering*, 13, 39-50 (2016).
- [14] Srinivasacharya, D., Mallikarjuna, B. and Bhuvanavijaya, R. Soret and Dufour effects on mixed convection along a vertical wavy surface in a porous medium with variable properties, *Ain Shams Engineering Journal*, 6, 553-564 (2015).
- [15] Srinivasacharya, D., & RamReddy, Ch. Soret and Dufour effects on mixed convection in a non-Darcy porous medium saturated with Micropolar fluid, *Nonlinear Analysis: Modelling and Control*, 16, 100-115 (2011).
- [16] Mishra, S. R, Baag, S. & Mohapatra, D. K. Chemical reaction and Soret effects on hydromagnetic micropolar fluid along a stretching sheet, *Engineering Science and Technology, an International Journal*, 19, 1919-1928 (2016).
- [17] Mohamed, R. A. & Abo-Dahab, S. M. Influence of chemical reaction and thermal radiation on the heat and mass transfer in MHD micropolar flow over a vertical moving porous plate in a porous medium with heat generation. *International Journal of Thermal Sciences*, 48, 1800-1813 (2009).
- [18] Olajuwon, B. I, Oahimire, J. I & Waheed, W. A. Convection heat and mass transfer in a hydromagnetic flow of a micropolar fluid over a porous medium, *Theoret. Appl. Mech.*, 41, 93-117 (2014).
- [19] Jat, R. N, Saxena, V. & Rajotia, D. MHD stagnation point flow and heat transfer of a micropolar fluid in a porous medium, *Journal of International Academy Physical Sciences*, 16, 315-328 (2012).
- [20] Pal, D. & Chatterjee, S. Heat and mass transfer in MHD non-Darcian flow of a micropolar fluid over a stretching sheet embedded in a porous media with non-uniform heat source and thermal radiation, *Commun Nonlinear Sci. Numer Simulat*, 15, 1843-1857.
- [21] Ibrahim, S. M. (2014). Effects of chemical reaction on dissipative radiative MHD flow through a porous porous medium over a nonisothermal stretching sheet, *Journal of Industrial Mathematics, Research*, 2014, 1-10 (2010).
- [22] Hamad, M. A. A., Uddin, M. J, & Ismail, A. I. Radiation effects on heat and mass transfer in MHD stagnation-point flow over a permeable flat plate with thermal convective surface boundary condition, temperature dependent viscosity and thermal conductivity, *Nuclear Engineering and Design*, 242, 194-200 (2012).
- [23] Mukhopadhyay, S. Effects of thermal radiation and variable fluid viscosity on stagnation point flow past a porous stretching sheet, *Meccanica*, 48, 1717-1730 (2013).
- [24] Kandasamy, R. & Muhaimin, I. (2010). Lie group analysis for the effect of temperature dependent fluid viscosity and thermophoresis particle deposition on free convective heat and mass transfer under a variable stream conditions, *Appl. Math. Mech. Engl. Ed.* 31, 317-328.
- [25] Pal, D. Mondal, H. Effects of temperature-dependent viscosity and variable thermal conductivity on MHD non-Darcy mixed convective diffusion of species over a stretching sheet, *Journal of Egyptian Mathematical Society*, 22, 123-133 (2014).
- [26] Jena, S. K. & Mathur, M. N. Similarity solutions for laminar free convection flow of a thermomicropolar fluid past a non-isothermal flat plate, *International J. Eng. Sci.* 19, 1431-1439 (1981).
- [27] Mukhopadhyay, S., Layek, G. C. & Samad S. A. Study of MHD boundary layer flow over a heated stretching sheet with variable viscosity, *International Journal of Heat and Mass Transfer*, 48, 4460-4466 (2005).
- [28] Bhattacharyya, K. & Layek, G. C. Similarity solution of MHD boundary-layer flow with

- diffusion and chemical reaction over a porous flat plate with suction/blowing, *meccanica* 47, 1043-1048 (2012).
- [29] Brewster, M. Q. *Thermal Radiative Transfer Properties*, Wiley, New York, NY, USA (1992).
- [30] Akinbobola, T. E. & Okoya, S. S. The flow of second grade fluid over a stretching sheet with variable thermal conductivity and viscosity in the presence of heat source/sink, *Journal of Nigeria Mathematical Society*, 34, 331-342 (2015).
- [31] Seddeek, M. A. & Abdelmeguid, M. S. Effects of radiation and thermal diffusivity on heat transfer over a stretching surface with variable heat flux, *Physics Letters*, 348, 172-179 (2006).
- [32] Dada, M. S. & Salawu, S. O. Analysis of heat and mass transfer of an inclined magnetic field pressure-driven flow past a permeable plate, *Application and applied Mathematics: An International Journal*, 12, 189-200 (2017).